Characterization of Implantable Microfabricated Fluid Delivery Devices

Ruben Rathnasingham [†], Daryl R. Kipke [†]
Sanford C. Bledsoe [‡], John D. McLaren [‡]

Submitted to IEEE Transactions on Biomedical Engineering
August 6th, 2002

[†] Neural Engineering Laboratory, Department of Biomedical Engineering, University of Michigan. [‡] Kresge Hearing Research Institute, University of Michigan
This work was supported by DARPA, grant number 885002, monitored by Dr. Eric Eisenstadt and by NIH-NIBIB, grant number EB00308.

Abstract - The formal characterization of the performance of microfluidic delivery devices is crucial for reliable *in-vivo* application. A comprehensive laboratory technique was developed and used to optimize, calibrate and validate microfabricated fluid delivery devices. *In-vivo* experiments were carried out to verify the accuracy and reliability of the pressure driven devices. Acute guinea pig experiments were conducted to measure the response to AMPA, an excitatory neurotransmitter, at multiple locations in the inferior colliculus. A non-dimensional parameter, $\widetilde{Q}$, was successfully used to classify devices in terms of geometry alone (i.e. independent of fluid properties). Functional devices exhibited long-term linearity and reliability in delivering single phase, Newtonian fluids, in discrete volumes with a resolution of 500 picoliters at less than 0.45 lbf/in^2 (30 mbar) pressure drop. The acute results showed a proportional increase in the firing rate for delivered volumes of 2 nL up to 10 nL (at rates of between 0.1 and 1 nL/s). Flow characteristics are maintained during acute experiments and post-implant. A control experiment conducted with Ringer solution produced negligible effects, suggesting the results to be truly pharmacological. The experimental techniques employed have proven to be reliable and will be used for future calibration and testing of next generation chronic microfluidic delivery devices.

I. INTRODUCTION

The physics of fluids has been studied in relation to physiology and biomedical instrumentation for many years. More recently, the advent of micro-fabrication technology and the potential impact of biotechnology and biomedical innovations have led to many novel ideas for manipulating fluids for drug discovery and delivery [1-3], diagnostics [4, 5], and combinatorial synthesis [6]. The prospect of lab-on-a-chip and *in-situ* drug delivery devices has brought the study of microfluidics to the forefront of device design and optimization. The advantages of microfluidic systems include the ability to work with small samples, the use of significantly smaller and less expensive chemical-analysis systems, and the combination of biosystems and more traditional electronic systems on a single substrate.

A breakthrough is being realized with the development of novel devices for accurately controlled drug administration. This technology has the potential of alleviating complications and therapeutic irregularities arising from the usual peak and trough pattern of drug concentration seen in single rapid-dosages [3, 7]. Other benefits have come in the form of pain-free micro-needles for subcutaneous delivery [8], needle-less delivery with biolistics [9], and real-time feedback control using integrated sensors [10].

A primary challenge for this new technology is that the fluid dynamics is made complex not only by micro-geometries but also by the use of far from ideal fluids. Fluid channels smaller than 100 μm in diameter result in laminar flow, which may simplify microfluidic modeling, but makes fluid mixing more difficult. Novel fluid-flow techniques, such as interleaving fluid channels and fluid lamination in multiple thin sheets, can be employed to help promote fluid mixing [11, 12]. Other challenges include: controlling the effects of surface tension, which can dominate in micro channels [13]; avoiding bubbles in micro channels; accurately measuring fluid flow [14, 15]; trapping particles in channels; slip effects [16]; and integrating fluidic components, such as micro pumps and flow meters [10].

An obstacle to the growth of this technology is fluid delivery performance and reliability. Experiments by Pfahler *et al.* [14], Ren *et al.* [15], Westin *et al.* [16] and Kittilsland *et al*. [17] clearly demonstrate the difficulties in working with microfluidic delivery. Pfahler *et al*. found flow rates that differed unpredictably when compared to standard theory for laminar flow without slip effects. They also report on channel plugging when attempting to use de-ionized water. Studies focused on electrokinetic effects using de-ionized water, and saline solutions were undertaken by Ren *et al*.. They report a substantial flow reduction due to electrokinetic forces when aqueous solutions with small ionic concentrations are used. Westin *et al.* performed careful experiments to calibrate fluid properties but encountered problems related to mass flow measurements and flow behavior. There is a clear need for a robust and effective calibration scheme for microfabricated fluid delivery devices that can account for different fluid properties and device geometry.

In the current study, the specific challenges of neural drug delivery probes are addressed. The particular flow issues here include the manipulation of very low volumes (nanoliters), discrete pulse delivery, and fluid diffusion in the neural environment. A systematic method to calibrate, test, and optimize fluid delivery devices is presented. The technique is generalized such that it can be used to calibrate passive fluid delivery probes or to calibrate flow meters that are incorporated into active probes. The experiments discussed in this paper extend the work done by Chen *et al.* [18], in which similar fluid delivery probes were used in *in-vivo* neural drug delivery. Further work by Papageorgiou *et al.* [10] showed the benefits of integrating flow meters into delivery devices, allowing for continuous measurements and real-time feedback. In their case, the flow meters are calibrated, and then used to measure instantaneous flow characteristics. The techniques described in the current study are applicable to both the calibration of flow devices and integrated flow meters.

The problem falls into two main categories: the characterization of the fluid and its behavior in micro-geometries, and the calibration of the delivery device. Key issues in microfluidics are briefly discussed before an experimental procedure for the calibration and testing of a fluid delivery probe is presented. Calibrated devices are then used in acute studies to validate *in-vivo* drug delivery performance.

II. CHARACTERIZATION OF FLUID SYSTEMS

A. Fluid Characterization

Fluids are first classified by phase conditions (homogeneous, pseudo-homogeneous or heterogeneous), secondly, by their time-dependent behavior when subjected to initial shear (thixotropic, viscoelastic), and finally by the main classes of flow behavior exhibited over limited ranges of shear rate under steady state shear (Newtonian, shear-thinning, shear-thickening, Bingham plastic, and viscoplastic). Most fluids used in biomedical applications behave as Newtonian fluids within certain ranges of shear stress, but tend to deviate from this behavior over a wider range. Non-Newtonian fluids exhibit a wide variation in behavior under stress. They do not obey Newton's law of viscosity and are characterized by the relationship of viscosity to the applied shear stress. Fluids must be characterized before their flow behavior in micro-geometries can be accurately modeled.

In this paper, the primary focus is the development of a robust calibration scheme that can be used with any fluid and device configuration. Multiple devices were used to validate the calibration scheme; however, only two Newtonian, single phase fluids (water and methanol) were used in this initial study. Experiments using colloidal and ionic solutions are currently underway. In the following section, flow characteristics associated with single and multi-phase fluids in micro-geometries are presented for completeness.

B. Flow Characterization

Microfluidics describes the movement, control, and measurement of fluids on a micrometer-to-millimeter scale. It involves the study of flow properties rather than the fluid properties discussed above. Microfluidic-related length scales are typically measured in micrometers and are used to deliver picoliters of fluid. In this flow regime, characteristics derived from generalized fluid dynamics are dominated by viscous forces and surface effects. The most important of these characteristics are summarized below:

(i) Inertia forces are normally small compared with viscous forces, and the equation of motion for the fluid reduces to the linear Stokes' form.
(ii) The movement of free particles due to thermal motion over characteristic time scales is often significant.
(iii) Colloidal particles settle out so that they may be considered to be suspended in the flow and moving with it. As a result, the principle concern is to determine the rheological properties of the colloidal suspension.
(iv) Interfacial surface effects are important due to the increased surface to volume ratios at micrometer scales.
(v) Solid and liquid particles typically acquire a charge in aqueous solution and electrokinetic effects become significant at these scales.

These characteristics are not mutually exclusive and may result in significant complications if not taken into account in the design of microfluidics systems. Note that the characteristics are both a function of the fluid (viscosity, surface tension, charged particles) and the device (geometry, surface chemistry).

C. Device Calibration

Typical internal dimensions of microfluidic devices produce Reynolds numbers much less than 1, resulting in laminar flow behavior. Non-dimensional analysis provides a simple relationship between applied pressure and volume flow rate. In this section, two theoretical formulations to describe the bulk flow characteristics of laminar flow channels are presented: one uses a theoretical relationship between pressure drop and flow velocity; and the other develops a non-dimensional volume flow rate parameter for a Newtonian, single-phase fluid. Shah and London [19] provide a conventional empirical expression used for laminar channel flows:

$$\Delta p = 30 \frac{\mu V l}{d^2}, \tag{1.1}$$

where μ is the fluid viscosity, d and l are length scales, V is the average cross-sectional flow velocity, and the pressure drop along the flow channel is Δp. Chen *et al.* [18] performed careful experiments with multiple microfabricated fluid delivery devices and found the constant of proportionality to be closer to 27.5. This relationship is compared to measured calibration results in the present study.

Using conventional non-dimensional analysis, the non-dimensional volume flow rate, $\tilde{Q}$, can be written as:

$$\tilde{Q}\left(\frac{d}{l}\right) = \frac{Q\mu}{d^2 l \Delta p}, \tag{1.2}$$

where Q is the dimensional volume flow rate. Equation 1.2 shows that the non-dimensional volume flow rate is a function of the ratio of length scales and hence will be constant for a given device. $\tilde{Q}$ represents a convenient parameter for the classification of delivery devices in terms of flow efficiency. Devices with higher values of $\tilde{Q}$ will require a lower driving force for a given flow rate. $\tilde{Q}$ may also be useful as a quality control parameter in batch fabricated devices.

III. EXPERIMENTAL SETUP AND ACUTE PREPARATION

A. Flow Calibration Station

For continuous flow applications, calibrating a fluid delivery device primarily refers to the formulation of a transfer function between the driving force (in this case, pressure) and the volume flow rate. However, in practice, continuous flow is often accompanied by the delivery of discrete volumes in periodic short bursts. In discrete delivery, other important characteristics come into play, namely, response time, linearity of delivery, steady state error, accuracy, and repeatability. This study focuses on calibration for both continuous flow and repeated delivery of a discrete volume of fluid.

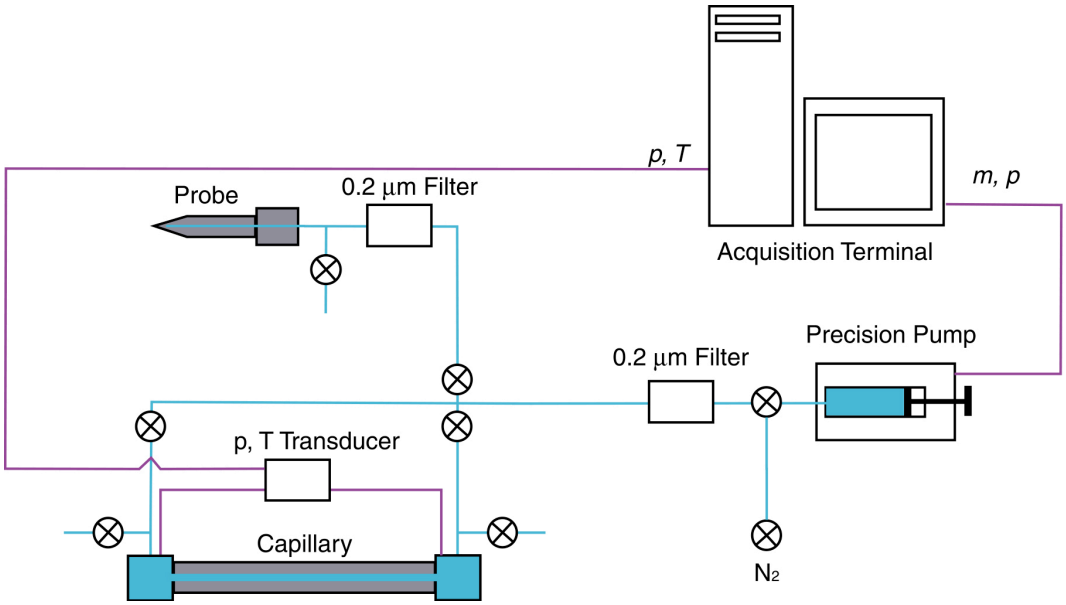

Figure 1: Schematic diagram of the flow calibration station illustrating bulk-flow fluid characterization and fluid delivery probe calibration. Two forms of driving forces are shown: pressure and electromotive current. N_2 is a nitrogen line-flushing source, m, p, T, i and c are the flow rate, pressure, temperature, current and conductance, respectively.

A custom designed flow calibration station is used to both characterize fluids and calibrate delivery devices (Figure 1). The flow is driven using a volume flow controlled syringe pump (WPI UltraMicroPump) and a micro syringe (Hamilton 0.5 μL 7000 series). The fluid is initially filtered through a 0.2 μm in-line filter (Corning, Inc.) to remove trace particulates. Solenoid-controlled micro-valves (Lee Company, Inc.) are used for the rapid control of flow direction throughout the circuit. Pressure is measured with a differential pressure transducer (Omega P26). A single shut-off valve is placed upstream of the probe to alleviate line pressure.

Mean pressure measurements are recorded using a standard desktop computer with a digital data acquisition system. Shut-off valves are operated with a manual switch box. A pressure test is conducted before every run to ensure seals are secure. This is done by sealing the exit ports of the system and raising the internal line pressure to 5 lbf/in^2 (350 mbar) for 15 minutes. A steady pressure must be maintained over this time. Filtered gas is used to flush the system after every calibration run. All experiments were carried out at room temperature.

As mentioned in the introduction, two separate tests are required: one for fluid characterization and another for device calibration. For fluid characterization, the pressure drop across a micro channel (Polymicro Inc. – 110 μm I.D., 10 cm long polyimide capillary) is measured at each flow rate (Figure 1). This allows for the characterization of non-ideal behavior of the bulk fluid by measuring the dynamic viscosity at different flow rates.

For the device calibration (flow characterization), a single pressure measurement is made immediately upstream of the probe and the fluid is dispensed into open atmosphere. In this case, appropriate values for viscosity, at given flow rates, are used with the measured pressure head loss through the probe to compute the value of $\tilde{Q}$ using Equation 1.2.

B. Discrete Volume Analysis

Typical drug delivery applications require short discrete bursts of fluid as well as continuous infusions. The characterization of burst behavior, however, cannot be reliably inferred from continuous pressure measurements due to the time lag between the application of pressure and flow response over the burst cycle.

Instead, flow injection analysis (FIA) is performed. With this technique, a discrete volume of a target compound (10^{-2} μM sodium salicylate in water) is injected into 130 μL of a carrier fluid (water). The mixture is then driven through a fluorimeter that computes the relative spectral concentration of the target compound. The FIA output is a spectrum with a spike at the emission frequency of sodium salicylate. The amplitude of the spike is a proportional measurement of the volume of sodium salicylate injected.

The FIA instrumentation includes a pump (Beckman 332), injector (Gilson Dilutor 401 and Autosampler 231), detector (SpectroVision FD-100 Filter Fluorimeter), and acquisition system (Shimadzu C-R4A Chromatopac Integrator). The excitation and

emission filters used in the fluorimeter have a center wavelength of 300 nm and a cut-off wavelength of 400 nm, respectively. These were chosen to correspond with sodium salicylate excitation and emission wavelengths of 308 nm and 430 nm, respectively.

C. Fluid Delivery Probe

The fluid delivery probe used in this study was designed and fabricated at the University of Michigan Center for Neural Communication Technology. It is a bulk-microfabricated, multi-channel silicon probe capable of selectively delivering chemicals at the cellular level as well as electrically recording from and stimulating neurons *in-vivo* [18]. The effective inner diameter of the single fluid channel is 25 μm, and the five recording sites are spaced 150 μm apart with the closest being 50 μm away from the channel exit (Figure 2). Each site is flush with the surface of the probe and has an area of 200 μm^2 – designed to function for both electrical recording and stimulation. The probe is mounted on a custom-built circuit board with integrated electrical connections. Access to the flow channel is provided through a polyimide tube and a glass capillary (Figure 3).

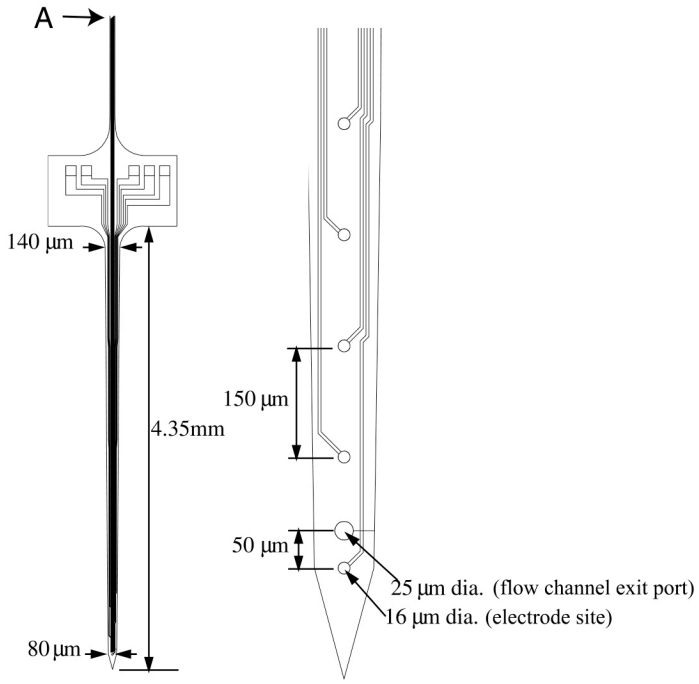

Figure 2: University of Michigan fluid delivery probe. The probe contains five independent electrodes and a single fluid delivery channel.

Large surface to volume ratios of microfabricated fluid channels result in significant surface tension effects. This is, in fact, a major effect in all microfluidic applications. Consequently, care must be taken to ensure that there are no exposed surfaces in the flow system. This includes bubbles, leaks, foreign particulates, and stationary volumes of fluid. Complete saturation of the flow system is ensured in these experiments by adopting

the following procedure: the probe is first back-filled with fluid using a vacuum pump system (Figure 3a); then a flexible polyimide tube (WPI MicroFil) is inserted into the

glass capillary until it makes contact with the upstream tip of the probe (point A in Figure 2 and 3a); next the capillary is filled; and finally the polyimide tube is gradually removed, to prevent leaving air bubbles behind.

A syringe assembly (Figure 3c) provides the required flow through the probe. The seal between the syringe and the glass capillary of the probe assembly is maintained with sticky wax. Figure 3d illustrates another delivery configuration that was preferred as it allows for flexibility in the positioning of the probe during insertion into the brain. The syringe needle is removed and replaced by a polyimide tube into which the plunger moves to displace the fluid. A rubber ferrule is used at the syringe-capillary junction to maintain a good seal while the seal around the glass capillary is made using sticky wax.

D. Acute Experiments

All acute experiments discussed here were conducted in a double-walled, sound attenuating booth. The probe was used to stimulate regions of the central nervous system of guinea pigs, which were anesthetized with ketamine hydrochloride (100 mg/kg, IM) and xylazine (20 mg/kg, IM). The animals were held in a stereotaxic device (Kopf), and rectal temperature was monitored and maintained at 38.5 °C with a thermostatically controlled heating pad. The skull was exposed and the bone over the cerebellum and posterior occipital cortex removed to provide dorsal access to the inferior colliculus (IC). The surface of the IC was exposed by aspirating the overlying occipital cortex. All procedures were performed under University of Michigan UCUCA approved protocols.

The probe was mounted on a custom-made holder with a micromanipulator for precise insertion. A 5 μM solution of α-amino-3-hydroxy-5-methyl-4-isoxalone propionic acid (AMPA) in Ringer solution was used in all fluid delivery experiments. The Ringer solution was composed of (in mM) NaCl, 145; KCl, 2.7; $CaCl_2$, 1.2; $MgSO_4$, 2.0; HEPES, 5.0, and had a pH of 7.3. The solution was expelled using a volume flow controlled syringe pump (WPI UltraMicroPump) and a micro syringe (Hamilton 0.5 μL 7000 series). This combination allows for a minimum flow volume of 26 pL. Dispensed fluid volumes ranged from 2 nL to 10 nL.

Changes in the response properties of isolated single units in the IC to local applications of AMPA, an excitatory analogue of L-glutamate, were investigated. AMPA was tested at concentrations of 5 μM (n = 5) and 10 μM (n = 5). It was expelled at volumes of 2 nL (0.2 nL/s, n = 2), 5 nL (0.5 nL/s, n = 6) and 10 nL (0.5 nl/s, n = 2). Volumes of Ringer solution alone were tested at 2 nL (n = 2) and 5 nL (n = 2). Action potentials, which were recorded using the five electrodes on the probe, were amplified and digitized by a multichannel data acquisition system (Plexon, Inc.). The system was programmed for on-line generation and visual display of post-stimulus time (PST) histograms and spike counts. PST samples (15 samples each) were recorded to obtain spontaneous activity before, during, and after drug infusion. Detailed analysis and hardcopy output of PST

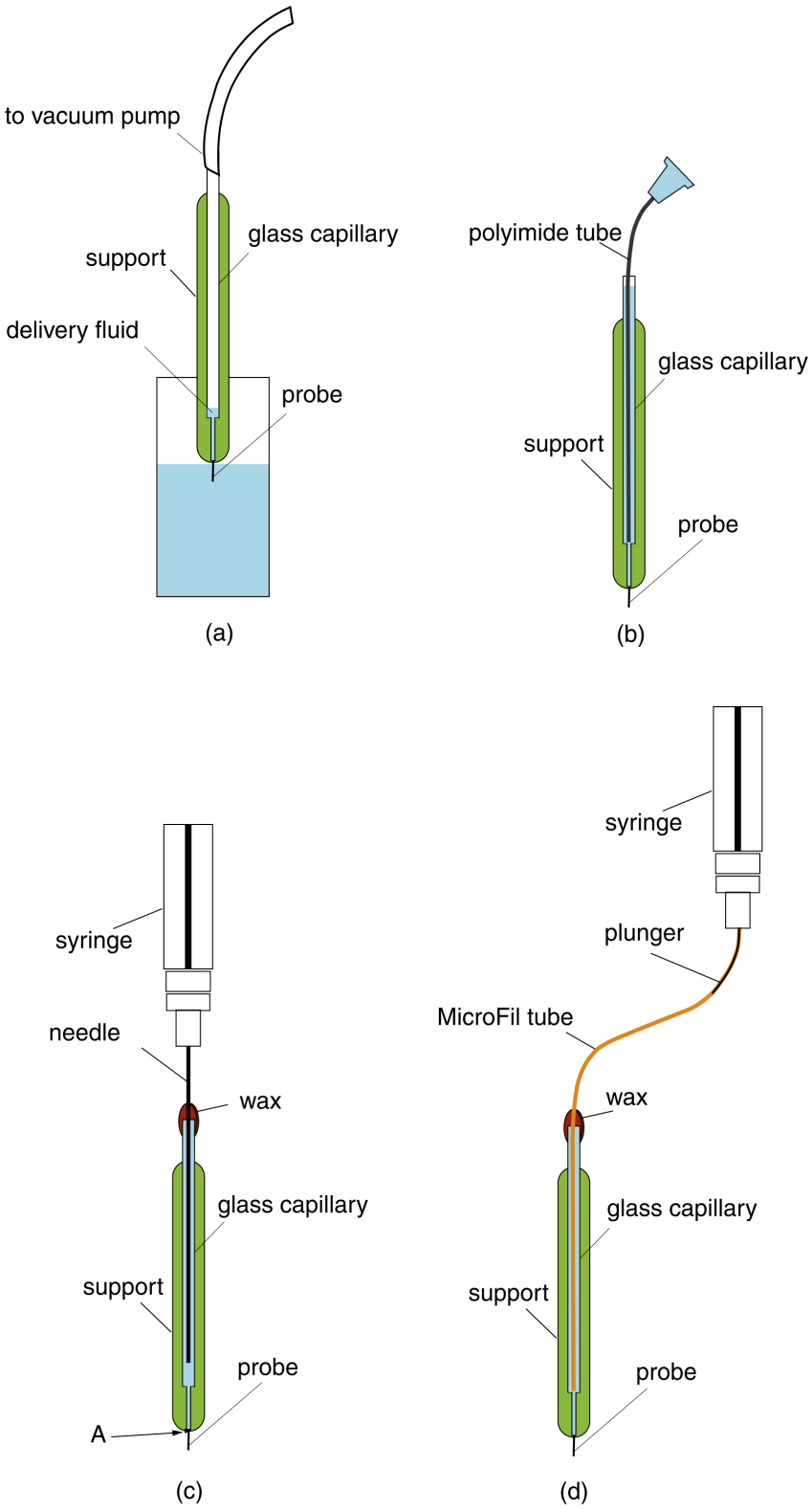

Figure 3: Preparation of probe prior to fluid delivery. (a) back-fill, (b) using a MicroFil polyimide tube to fill glass capillary, (c) syringe and probe assembly, (d) syringe and polyimide assembly.

histograms were performed off-line using Neuroexplorer software. Electrical recordings were obtained only from animals in a stable physiological state as monitored by heart rate and/or respiration. The control experiment was conducted with the Ringer solution alone.

IV. RESULTS

A. Device Calibration

The proportionality between pressure drop and volume flow rate is provided by the calibration results plotted in Figures 4a and 4b. Figure 4a shows the cumulative results for four different probes tested with de-ionized water at room temperature. As expected, greater errors are found at the lowest flow rates due to pump instabilities. Corresponding theoretical values derived from Equation 1.1 are plotted in Figure 4a to show the deviation of the measured data from theory (an error of 14% in the average slope). Figure 4b shows the result from a single probe using two different fluids: de-ionized water and methanol. The slope of the data for methanol decreases by 54%, corresponding to the theoretical reduction in viscosity of 60% compared to water.

Calibrations from seven independent devices resulted in an average value for $\tilde{Q}$ of 1.2 x10^{-7} with a variability of approximately 10%, suggesting fabrication and packaging improvements may be necessary for better quality control between device batches. Each device demonstrated repeatability with errors in $\tilde{Q}$ of less than 5 %. This repeatability was maintained post-implant.

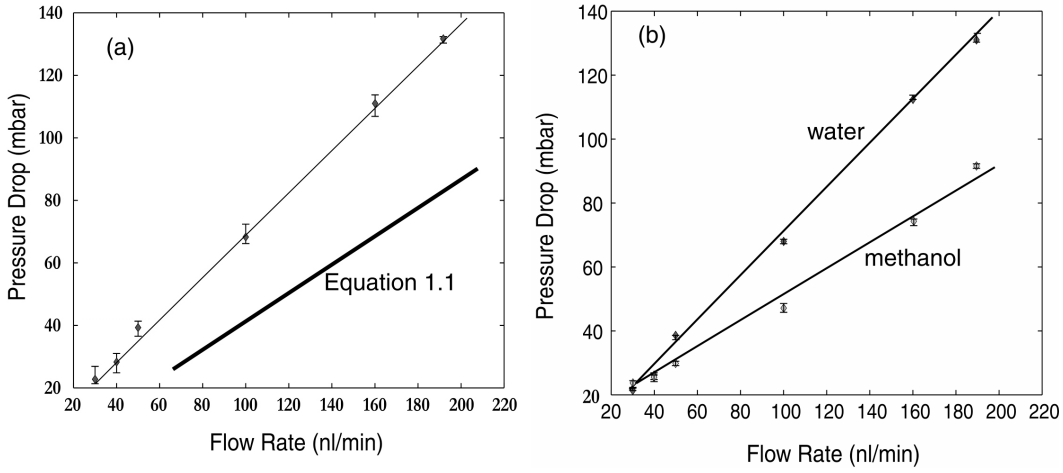

Figure 4: Calibration results showing linearity and repeatability for (a) four independent probes and corresponding laminar flow theory (Equation 1.1) and (b) different fluids: water and methanol.

B. Flow Injection Analysis

Flow injection analysis provides a constant of proportionality for discrete volume fluid delivery (Figure 5). The amplitude taken from the output spectrum corresponds to the fluorescent peaks of sodium salicylate. The discrete volumes (ranging from 1 to 26 nL) were injected at a constant flow rate spanning a range of delivery times from 25 ms to 510 ms.

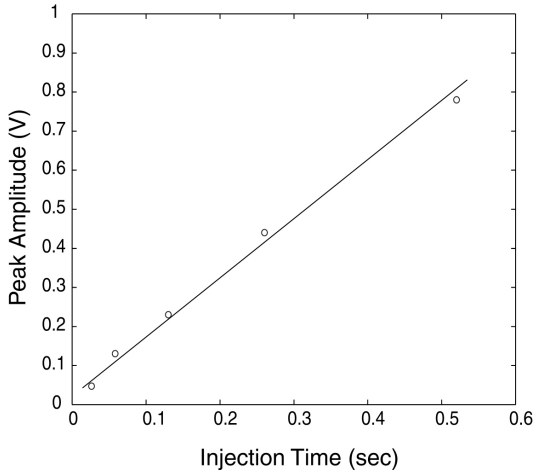

Figure 5: Plot of injected volume against FIA peak value for sodium salicylate, illustrating the linearity of discrete volume injections.

C. Neural Response

The efficacy of the drug-delivery system was tested *in-vivo* on neural discharge in the inferior colliculus of the guinea pig brain in three experiments. In 9 of the 10 applications of AMPA, there was a clear excitatory effect that was rapidly seen at all 5 recording sites using the volumes tested , which are large relative to the volumes of cells. Figure 6a shows the effects of a 5 nL application of 5 □M AMPA on neural discharge at five sites recorded simultaneously in the inferior colliculus. Site 1 was located 50 □m above the drug-delivery orifice while the other four sites were spaced at 150 □m increments above Site 1 (Figure 2). Each data point represents 10 seconds of neural activity. The application of AMPA produced excitation that began during the first 10-second epoch at each of the five sites and the excitation lasted for 50-60 seconds. Figure 6b shows results obtained with an equivalent control application of Ringer solution alone (5 nL in 10 s). The neural discharge rate was transiently suppressed for about one min at all the sites except Site 5 which was the furthest from the channel orifice. A suppression of activity was commonly observed at high volumes (5 nL in 10 s and 10 nL in 20 s) but not at a lower volume (2 nL in 10 s, Figure 7b). Figure 7a shows the effects of a 2 nL application of 5 □M AMPA. Although excitation still occurred rapidly at all 5 five recording sites, the excitation was more transient with this smaller volume lasting only 10-20 seconds.

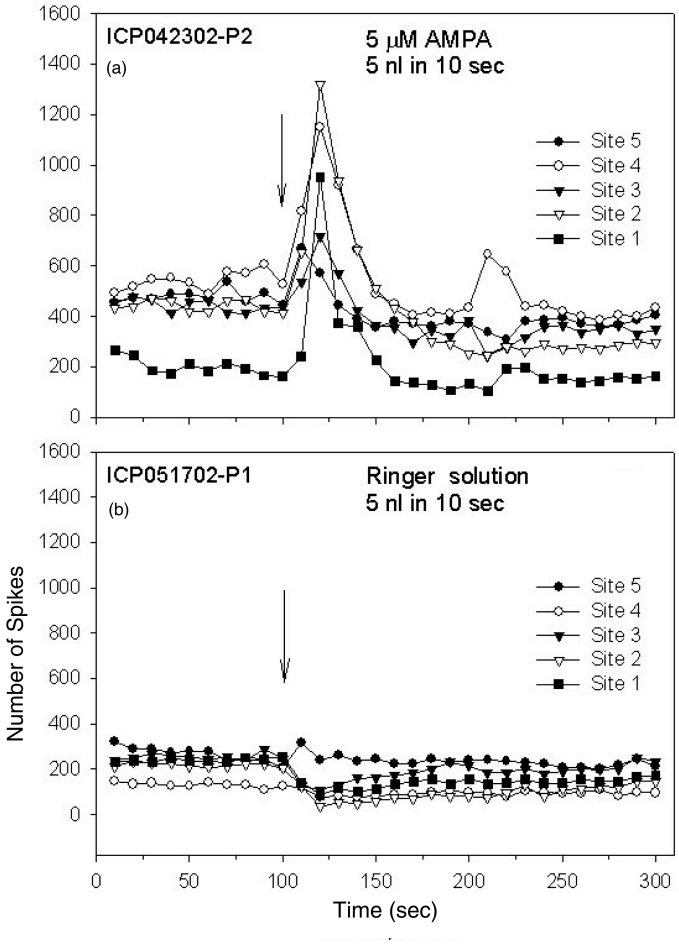

Figure 6: Neural discharges from five recording sites in the inferior colliculus of a guinea pig before and after ejection of (a) 5 μM AMPA (5 nL in 10 s) and (b) Ringer solution alone (5 nL in 10 seconds). Each data point represents 10 s of neural activity. The arrow denotes the time of ejection.

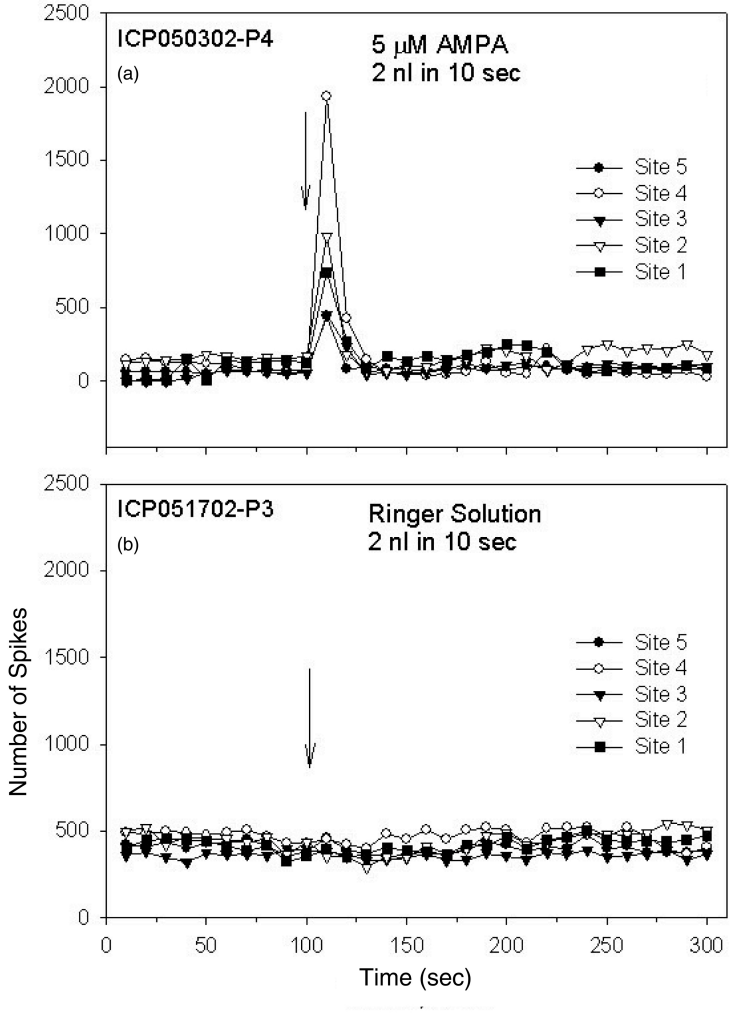

Figure 7: Neural discharges from five recording sites in the inferior colliculus of a guinea pig before and after ejection of (a) 5 □M AMPA (2 nL in 10 seconds) and (b) Ringer solution alone (2 nL in 10 seconds). Each data point represents 10 seconds of neural activity. The arrow denotes the time of ejection.

V. DISCUSSION

The calibration results and acute animal experiments address key issues in microfluidic systems:

(i) The consistent results among different batches of microfabricated devices (Figure 4a) and the repeatability of a single probe (Figure 4b) point to a robust fabrication process that leads to channel walls with mechanical integrity and flow paths that are free of spurious contaminants. This is a common problem in microfabricated flow channels and a robust, repeatable fabrication process is of primary concern in producing reliable fluid delivery devices.

(ii) Although the devices exhibited linear flow behavior, the absolute relationship between pressure drop and flow rate was not accurately predicted by laminar theory given by Equation 1.1. This discrepancy, shown in Figure 4a, stems mainly from entrance and surface losses throughout the probe flow line that cannot be accurately taken into account due to current fabrication and packaging irregularities. Accurate calibration procedures, as those described in this paper, are necessary to determine these losses and establish true device characteristics.

(iii) Figure 4b illustrates the dependence of device performance with fluid properties. The result demonstrates the value of independent device calibration and fluid characterization procedures to extract the effects of the fluid properties. Greater effects are expected with non-Newtonian fluids and colloidal solutions. The results also demonstrate the value of using $\widetilde{\boldsymbol{Q}}$ when delivering Newtonian fluids since its value remains constant with different fluid properties and thus may be used to classify families of devices.

(iv) The robustness of the probe is also seen in the delivery of discrete volumes of fluid (Figure 5). The reliable delivery of very small flow volumes (less than 1 nl) supports a diverse set of applications from neurotransmitter delivery, where individual neurons are targeted, to therapeutic drug delivery, where regions of cortex are effected. The acute animal studies (Figures 6 and 7) further demonstrate the potential of this technology to elicit pharmacological effects localized in space and time.

(v) For *in-vivo* fluid delivery, the bulk flow of fluid at larger volumes would be expected to produce greater mechanical effects such as pushing cells away and having greater effects on current fields altering the electrical properties of the cells. This was sometimes observed as a reduction in neural spike amplitude and changes in signal-to-noise ratios. Thus, it is important to utilize low volumes to obtain unbiased and reliable data in response to drugs. The response would be expected to be less influenced by the effects of bulk flow of fluid at lower volumes (Figure 7b), but it is apparent that if smaller volumes are used, higher concentrations of drugs will be required.

(vi) The reliable delivery of small discrete volumes is crucial when considering future applications in neural drug delivery. The enabling technology will come in the form of implantable, chronic devices. Packaging designs for the chronic version of the current device and the development of next generation, multiple-channel drug delivery devices are presently underway. The drug delivery aspect of these devices will include a reservoir of fluid that is

delivered in discrete, programmable volumes over time. Fast-acting microvalves, whose operation will be determined by the discrete volume characteristics described above, will control the flow. This discrete volume calibration is thus a vital element in the development and application of chronic devices.

The experimental techniques developed in the current study have proven to be useful tools in highlighting important characteristics of microfluidic delivery devices and allow the formal identification of their performance. Successful *in-vivo* experiments confirm the suitability of probes as robust implantable fluid delivery devices.

VI. CONCLUSION

A custom designed calibration setup was successfully used to calibrate fluid delivery probes over their designed flow rates (0.1 to 1 nl/s). A quality control parameter, $\tilde{Q}$, was used to qualify the performance of a device and confirmed the repeatability of the tested probes. The probes exhibit a steady linear behavior for both continuous and discrete injections indicating a robust fluid delivery channel free of random irregularities. Acute experiments succeeded in demonstrating the *in-vivo* reliability of the probe as a hybrid fluid delivery/electrical recording device. The results further highlight the sensitivity of neuronal responses to fluid volume and establish an upper boundary beyond which physical displacement of cells take place and electrical recordings become unpredictable. The probes successfully deliver biologically appropriate doses of solution in the cortical environment.

VII. ACKNOWLEDGEMENT

The authors would like to thank Jim Grotberg, Shuichi Takayama, Jamille Hetke, Kensall Wise, David Anderson and David Pellinen for numerous helpful discussions. The fluid delivery probes were provided by the University of Michigan Center for Neural Communication Technology sponsored by NIH/NCRR grant P41 RR09754

REFERENCES

[1] R. J. Mariella, "MEMS for Bio-Assays," *Biomedical Microdevices*, vol. 4, pp. 77-87, 2002.

[2] P. Dario, Carrozza, M.C., Benvenuto, A., Menciassi, A., "Micro-Systems in Biomedical Applications," *J. Micromech. Microeng.*, vol. 10, pp. 235-244, 2000.

[3] J. T. Santini, Cima, M. and Langer, R., "A Controlled Release Microchip," in *Nature*, 1999, pp. 335-338.

[4] M. A. Burns, Johnson, B.N., Brahmasandra, S.N., Handique, K., Webster, J.R., Krishnan, M., Sammarco, T.S., Man, P.F., Jones, D.K., Heldsinger, D., Mastrangelo, C.H., Burke, D.T., "An integrated nanoliter DNA analysis device," in *Science*, vol. 282, 1998, pp. 484-487.

[5] D. T. Burke, Burns, M.A., Mastrangelo, C.H., "Microfabrication Technologies for Integrated Nucleic Acid Analysis," *Genome Research*, vol. 7, pp. 189-202, 1996.

[6] T. Fujii, Hosokawa, K., Nojima, T., Shoji, S., Yotsumoto, A. Endo, I., "Microfabricated reactor for cell-free protein synthesis," presented at Proceedings of the 1997 19th Annual International Conference of the IEEE Engineering in Medicine and Biology Society, Chicago, IL, 1997.

[7] J. Urquhart, "Controlled Drug Delivery: Therapeutic and Pharmacological Aspects," *Journal of Internal Medicine*, vol. 248, pp. 357-376, 2002.

[8] D. V. McAllister, Allen, M.G., Prausnitz, M.R., "Microfabricated Microneedles for Gene and drug Delivery," *Annu. Rev. Biomed. Eng.*, vol. 2, pp. 289-313, 2000.

[9] M. A. F. Kendall, Wrighton Smith, P.J., Bellhouse, B.J., "Transdermal ballistic delivery of micro-particles: Investigation into skin penetration," presented at Annual International Conference of the IEEE Engineering in Medicine and Biology, 2000.

[10] D. Papageorgiou, Bledsoe, S.C., Gulari, M., Hetke, J.F., Anderson, D.J., Wise, K.D., "A Shuttered Probe with In-Line Flowmeters for Chronic In-Vivo Drug Delivery," presented at Digest IEEE Microelectromechanical Systems Conference, Interlaken, 2001.

[11] J. Evans, Liepmann, D., Pisano, A. P., "Planar laminar mixer," presented at Proceedings of the IEEE Micro Electro Mechanical Systems (MEMS), Piscataway, NJ, 1997.

[12] D. Liepmann, Evans, J., D., "Micro-Fluidic Mixer," presented at Polymeric Materials Science and Engineering, Proceedings of the ACS Division of Polymeric Materials Science and Engineering, Washington, DC, 1997.

[13] C. J. Kim, "Microfluidics using the surface tension force in microscale," presented at Proceedings of SPIE - The International Society for Optical Engineering, Bellingham, WA, 2000.

[14] J. Pfahler, Harley, J., Bau, H., Zemel, J., "Liquid Transport in Micron and Submicron Channels," *Sensors and Actuators*, pp. 431-434, 1990.

[15] L. Ren, Li, D., Qu, W, "Electro-viscous effects on liquid flow in microchannels," *J. Coll. Interface Sci.,*, vol. 233, pp. 12-22, 2001.

[16] K. J. A. Westin, Breuer, K.S., Choi, C.H., Huang, P., Cao, Z and B. Caswell, Richardson, P.D., Sibulkin, M., "Liquid Transport Properties in Sub-Micron Channel Flows," presented at Proceedings of 2001 ASME International Mechanical Engineering Congress and Exposition, New York, NY, 2001.

[17] G. Kittilsland, Stemme, G., Norden, B., "Sub-Micron Particle Filter in Silicon," *Sensors and Actuators*, vol. 23, pp. 904-907, 1990.

[18] J. K. Chen, Wise, K.D., Hetke, J.F., and Bledsoe, S.C. Jr., "A Multichannel Neural Probe for Selective Chemical Delivery at the Cellular Level," *IEEE Transactions on Biomedical Engineering*, vol. 44, 1997.

[19] R. K. Shah, London, A.L., *Laminar Flow Forced Convection in Ducts*. New York: Academic, 1978.